

Impact of Environmental Conditions on the Remaining Useful Lifetime of SiC MOSFET

Md Zakir Hasan
*Department of Electrical and Computer Engineering
 Mississippi State University
 Starkville, USA
 mh3482@msstate.edu*

Ashik Amin
*Department of Electrical and Computer Engineering
 Mississippi State University
 Starkville, USA
 aa2719@msstate.edu*

Md Moniruzzaman
*Department of Electrical and Computer Engineering
 Mississippi State University
 Starkville, USA
 mm5111@msstate.edu*

Seungdeog Choi
*Department of Electrical and Computer Engineering
 Mississippi State University
 Starkville, USA
 seungdeog@ece.msstate.edu*

Prashant Singh
*Department of Mechanical, Aerospace & Biomedical Engineering
 University of Tennessee
 Knoxville, USA
 psingh15@utk.edu*

Chun-Hung Liu
*Department of Electrical and Computer Engineering
 Mississippi State University
 Starkville, USA
 chliu@ece.msstate.edu*

Abstract— Silicon carbide (SiC) power MOSFETs are widely applied to critical infrastructure in modern energy systems. Thus, accurately predicting its remaining useful lifetime (RUL) in real-world applications has become crucial. State-of-the-art explored its RUL through a power cycling test mostly under fixed or without considering environmental conditions (e.g., fixed temperature and humidity). This has resulted in considerable RUL prediction errors in real-world applications. To address this gap, this study directly integrates environmental factors into the RUL modeling. Specifically, the junction temperature (T_j), on-state voltage ($V_{ds, on}$), on-state resistance ($R_{ds, on}$), and case temperature (T_c) have been explored in various environmental conditions to understand their tight correlations with the RUL in the real world. Time series statistics models Autoregressive (AR) and Autoregressive Integrated Moving Average (ARIMA) have been used to predict SiC MOSFET RUL to gain new insights systematically.

Keywords— *SiC MOSFET, Lifetime, Junction Temperature, Environmental Conditions, Time series model*

I. INTRODUCTION

The continuous evolution of technology is driving a significant rise in the demand for power electronics across a wide range of applications. While Si MOSFETs and IGBTs have long been the workhorses of this domain, a new wave of wide bandgap (WBG) power electronics switches, notably silicon carbide (SiC) MOSFETs and gallium nitride (GaN) FETs, is rapidly gaining traction. The ascendancy of WBG materials like SiC can be attributed to their inherent superior electrical properties [1] compared to Si shown in Fig. 1. Especially the SiC MOSFET power module offers several advantages compared to the discrete SiC MOSFET (e.g., enhanced power density, improved thermal management, and higher operating temperature).

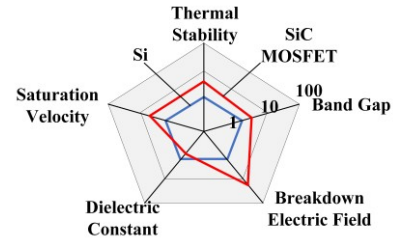


Fig. 1. Properties comparison between Si and SiC power switches.

Power devices are simultaneously exposed to time-varying environmental conditions like high temperatures and humidity. In such environments, where they endure prolonged electrothermal stress, these devices may degrade earlier, potentially impacting the system's overall reliability. Standard power cycling test only considers electrothermal stress and ignores the effect of temperature or humidity from the environment. However, the failure rate, λ of the SiC MOSFET, is closely related to the environmental conditions [2] and the load conditions. The failure rate depends on the environmental conditions as follows:

$$\lambda = \lambda_{ref} \cdot \pi_A \cdot \pi_Q \cdot \pi_E \quad (1)$$

where the failure rate λ depends on environmental factors, π_E (e.g., temperature or humidity), could accelerate the degradation. Especially, the environmental factors, π_E (e.g., temperature or humidity), could impact the degradation precursors (e.g., on-state voltage, on-state resistance, gate-source threshold voltage, rise time, delay time, or junction temperature), significantly resulting in the lifetime change of SiC switches [3]. Humidity [4] influences the lifetime of SiC MOSFETs. SiC MOSFETs characteristics heavily depend on the junction temperature [5]. If junction temperature varies, then the characteristics will also be changed. The environmental

temperature will impact the junction temperature deviation, eventually evolving the characteristic and impacting RUL. However, state-of-the-art mostly explores RUL with fixed power cycling tests without modeling such a crucial environmental impact. This has resulted in considerable errors in real-world RUL prediction.

There are many methods to determine the lifetime of SiC MOSFETs. One is the power cycling test, in which the lifetime of SiC MOSFETs can be achieved quickly [6]. The on-state resistance ($R_{ds, on}$) is widely used as the aging and degradation indicators of SiC MOSFETs [7]. However, threshold voltage (V_{th}), drain current (I_d), rise time (t_r), and fall time (t_f) are also used as the precursor for determining the lifetime of SiC MOSFETs [8-9]. The on-state resistance value depends on the junction temperature. With the junction temperature increase, the bond wire resistance (R_{bw}) of SiC is increased, which is part of on-state resistance.

For aging and degradation, junction temperature deviates on-state resistance. Thus, junction temperature needs to be measured or estimated precisely. To estimate T_j , using Thermosensitive Electrical Parameters (TSEPs) is one of them [10-11]. TSEPs include on-state voltage, threshold voltage, gate resistance, etc. However, this approach is not fully accurate because the relationship between TSEPs and T_j can vary under different power converter load conditions. Also, measuring TSEP requires an additional measurement circuit. Many practitioners use only the case temperature (T_c) to estimate the junction temperature, but this method is not precise, especially at high currents and power injections. The discrepancy between case and junction temperatures becomes significant, highlighting the need for a more accurate method to estimate the junction temperature and determine the Remaining Useful Life (RUL) [12-13].

There are physical models and data-driven prediction methods. Physical models such as the Coffin-Manson and Bayer models are used for the lifetime prediction of SiC MOSFETs. These models have low accuracy and are less efficient [14]. Data-driven methods estimate lifetime based on the available data, which is more accurate and efficient.

This paper aims to determine the influence of temperature on the lifetime of SiC MOSFETs. $R_{ds, on}$, T_j , and T_c will be measured as precursors for SiC MOSFET. Specifically, the environment correlation factors will be precisely modeled based on the $R_{ds, on}$ variation through power cycling tests under various temperature conditions. Then, the probability density functions and maximum log-likelihood will evaluate the correlation factors among different environmental conditions. The proposed method utilizes the trajectory of $R_{ds, on}$ based on projection and RUL estimation, using AR and ARIMA models. These models fundamentally depend on historical data to estimate their parameters and make predictions. These models integrate data-driven insights with model-driven principles. SiC MOSFET power modules have been analyzed through a DC power cycling test. The lifetime of SiC MOSFETs will be compared with different ambient environment temperatures. This proposed method offers a novel method to determine RUL in different environmental conditions, a practical method to measure the real-world RUL accurately.

The structure of this paper is organized as follows. Section II introduces the analysis of junction temperature estimation of SiC MOSFET. Section III provides RUL predictions of SiC MOSFETs. In section IV, simulation results are provided. Section V provides an experimental study, and section VI gives results and a discussion. Finally, Section VII summarizes this paper.

II. ANALYSIS OF JUNCTION TEMPERATURE ESTIMATION OF SiC MOSFET

The state-of-the-art assumes the fixed environment conditions or neglects the effects of humidity and temperature from the environment, which causes significant errors [15]. This paper explicitly models the impact of temperature from the environmental conditions, which will be integrated into the RUL prediction, as shown in Fig. 2. For the lifetime prediction, junction temperature estimation is necessary. The on-state resistance of SiC MOSFET has an impact on the varying junction temperature.

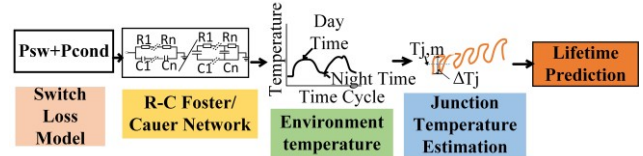


Fig. 2. SiC Switch RUL estimation mapping.

Commonly, junction temperature can be estimated by the Foster/Cauer network-based RC thermal impedance model. Fig. 3. shows an RC Foster network, which provides an efficient method to estimate junction temperature. However, this method cannot update associated changes in thermal impedance under various environmental conditions. Temperature-sensitive electrical parameter (TSEP) based methods estimate junction temperature with dynamic operating conditions. In this paper, FF33MR12W1M1HP_B11 is taken for the experiment. It has four layers of RC network, as provided in Table I. From the TSEP-based output, measuring parallel case temperature helps estimate junction temperature.

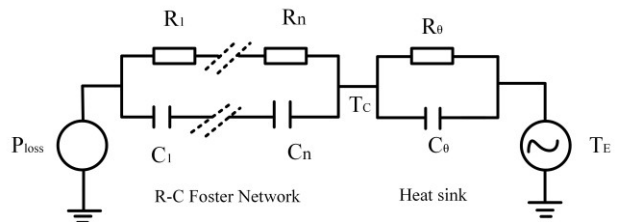


Fig. 3. RC Foster Network-based thermal modeling of the power switch module.

| TABLE I. RC VALUES FOR FOSTER NETWORK | | |
|---------------------------------------|---------|----------|
| Layers | R (K/W) | C (J/K) |
| 1 | 0.076 | 8.29E-03 |
| 2 | 0.221 | 0.0305 |
| 3 | 0.453 | 0.0801 |
| 4 | 0.81 | 0.1987 |

The input of Fig. 3 is the power loss of SiC MOSFET, and the output is junction temperature. Environment temperature is

considered the heatsink temperature for this model. The equivalent impedance of this network is as follows:

$$Z_{th}(t) = \sum_{i=1}^i C_i R_i (1 - e^{-R_i C_i}) \quad (2)$$

where Z_{th} is the equivalent impedance of the RC network, R_i and C_i are the thermal resistance and capacitance of the i_{th} layer of the foster RC network, respectively.

Junction temperature is the function of switch loss, which can be predicted through the R-C Foster/Cauer model [16] as follows:

$$T_j(t) = T_C(t) + P_{loss}(t)Z_{th}(t) \quad (3)$$

where P_{loss} is the switch loss, and T_C is the case temperature. Based on this equation, this model is efficient in estimating junction temperature. However, it cannot update itself due to the influence of environmental temperature and humidity.

As the environmental temperature has been considered for heatsink temperature, heatsink impedance also needs to be reconsidered for thermal modeling. In Fig. 3, thermal modeling can be calculated as a transfer function where T_E is the variable environment condition. Thermal impedance, Z_{th} as follows:

$$Z_{th}(s) = \frac{R_i}{R_i C_i s + 1} + \frac{R_\theta}{R_\theta C_\theta s + 1} \quad (4)$$

where R_θ and C_θ are the heatsink resistance and capacitance, respectively. In time series,

$$Z_{th}(t) = \frac{1}{C_i} e^{-R_i C_i t} + \frac{1}{C_\theta} e^{-R_\theta C_\theta t} \quad (5)$$

Thus, the equation (3) can be modified as follows:

$$T_{j,i}(t) = T_C(t) + P_{loss}(t)Z_{th,i}(t) \quad (6)$$

equivalent impedance, $Z_{th,i}(t)$ will change with the change of environmental temperature. With the varying environmental temperature, junction temperature will change. So, there is a tight relation between junction and environment temperature if all the other terms and load conditions are fixed. This relation can be called an environmental coupling factor (ψ).

$$T_{j,u}(t) = \psi(T_{j,f}(t)) + e_i(t) \quad (7)$$

where $T_{j,u}(t)$ is the updated junction temperature considering environmental conditions, $T_{j,f}(t)$ is fixed junction temperature without considering environmental conditions and $e_i(t)$ is the measurement noise error. Fig. 4 shows the junction temperature estimation of SiC MOSFETs, considering environmental conditions.

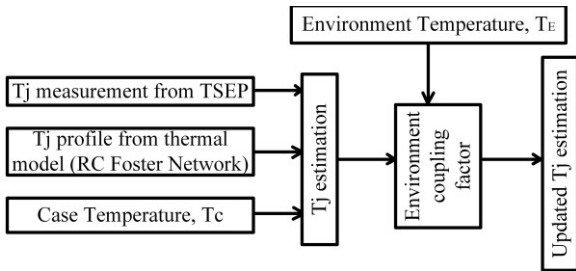


Fig. 4. Junction Temperature estimation for SiC MOSFETs.

The degradation acceleration factor (DAF) when the operating junction temperature ΔT_j changes due to environmental temperature can be defined as follows:

$$DAF = \left(\frac{\Delta T_{j,1}}{\Delta T_{j,2}} \right)^{-\beta} * \exp \left| \left(\frac{\gamma}{T_{j1,m} + 273} - \frac{\gamma}{T_{j2,m} + 273} \right) \right| \quad (8)$$

where $T_{j,m}$ is the minimum junction temperature, and ΔT_j is the junction temperature swing. β and γ are the empirical coefficients. In this case, β and γ will determine depending upon the characteristics (on-state voltage, on-state resistance) that change with the junction temperature. The DAF value will vary if junction temperature values are not the same. With the varying environmental conditions, the DAF value will change, and it eventually changes the lifetime of the SiC.

III. RUL PREDICTION OF SiC MOSFET

If DAF is increased or decreased, the time to reach the critical value (N_f) will be reduced or increased to degrade. Thus, the RUL is estimated as follows: $RUL = N - N_f$, where N is the total cycle time of the switch, and N_f is the number of cycles to reach its critical value [17-18]. N_f is utilized to calculate RUL in Fig. 5 by measuring the on-state resistance to address deviations resulting from various operating conditions. So, by determining $R_{ds,on}$ in various conditions, RUL is estimated using the time series autoregression (AR) and Autoregressive Integrated Moving Average (ARIMA) models.

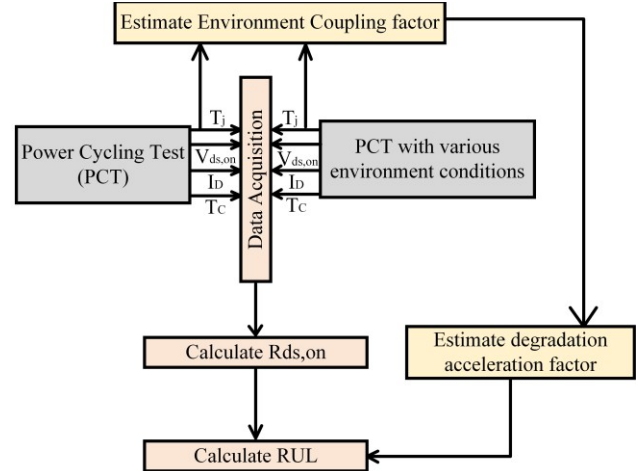


Fig. 5. Algorithm for estimating RUL of various environment conditions

The mathematical form of the AR model is:

$$R_{ds, on, n} = \sum_{i=1}^n \varphi_i R_{ds, on, n-i} + e_n \quad (9)$$

where φ is the model parameter, and e is the noise error. In this model, the output variable depends on its previous values and a white noise error. This statistical model is based on two steps. One is the prediction step, and another is the correction step. The trajectory of $R_{ds, on}$ can be estimated as follows:

$$R_{ds, on, p, n} = f(R_{ds, on, p, n-1}) + e_{n-1} \quad (10)$$

$$R_{ds, on, a, n} = g(R_{ds, on, p, n}) + m_n \quad (11)$$

where, $R_{ds,on,p,n}$ is the predicted $R_{ds,on}$ at time n, $R_{ds,on,a,n}$ is the experimental value $R_{ds,on}$ at time n, e is the process error, and m is the measurement error. These models are updated when new experimental data are available.

Another model is the ARIMA model, which works better for non-stationary rather than stationary data. The ARIMA model is a comprehensive model for time series data that can handle non-stationary data through differencing and incorporate autoregressive and moving average components. It has three parts: Autoregressive (AR), Integrated (I), and Moving Average (MA) part. The first part involves the regression of the output on its past output values, denoted by p . The second part differs past and present values to make it stationary, denoted by d , and the last part models the error term as a linear combination denoted by q . The mathematical form of the ARIMA model is as follows:

$$R_{ds,on,n} = c + \sum_{i=1}^p \varphi_i R_{ds,on,n-i} \sum_{j=1}^q \theta_j e_{n-j} + e_n \quad (12)$$

where c is the constant term, φ_i is the autoregressive coefficients, and θ_j is the moving average coefficients. This model can be effectively applied to non-stationary time series data. If $R_{ds,on}$ is stationary, the AR model is effective, but for non-stationary, the ARIMA model is more effective. In the result & discussion section, these two models are evaluated and compared to determine which is more effective.

IV. SIMULATION RESULTS

The DC power cycling test circuit with the cooling system parameters used in the PSIM software in Table II for simulation.

TABLE II. SIMULATION SYSTEM PARAMETERS

| Parameter | Value |
|---------------------------|------------------|
| SiC switch model | FF23MR12W1M1_B11 |
| V_{dc} (Supply Voltage) | 10 V |
| Load current, I_{Load} | 45 A |
| R_{load} | 0.2 Ω |
| Switching Frequency | 10 kHz |
| V_{GS} | 20/-5V |
| R_o (Thermal Interface) | 0.10 Ω |
| Thermal mass, C | 1 μF |
| R_θ (Heatsink) | 0.15 Ω |

Fig. 6 and 7 show the junction temperature variation in the same load conditions by imposing various environmental conditions in the test circuit.

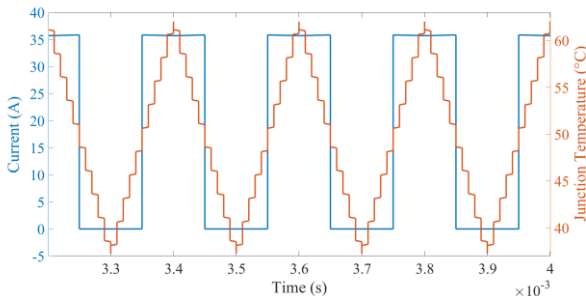


Fig. 6. Junction Temperature variation in 25~50-degree environment conditions.

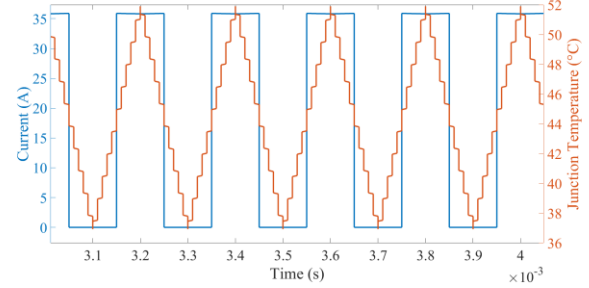


Fig. 7. Junction Temperature variation in 25~40-degree Celsius environment conditions.

The junction temperature data for different environmental conditions is taken from the experiment results. Normal, Gamma, and Weibull are considered to fit the junction temperature distribution. From the best-fitted distribution, the mean and variation of junction temperature is estimated, and it is observed that any deviation of junction temperature is under different environmental conditions. From the data set, the best fits using MATLAB are shown in Fig. 8 and Fig. 9, and the corresponding Log Likelihood of Normal, Gamma, and Weibull distributions are shown in Tables III, IV, and V.

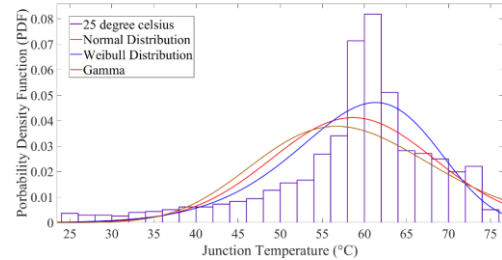


Fig. 8. Distribution fitting of 25-degree Celsius conditions data.

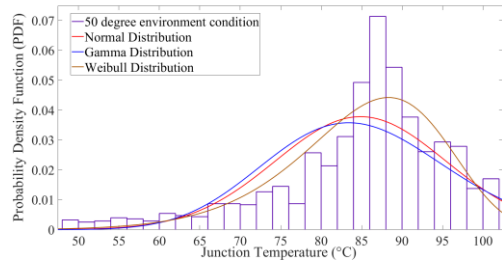


Fig. 9. Distribution fitting of 50-degree Celsius conditions data.

TABLE III- LOG LIKELIHOOD AND PARAMETERS FOR 25 °C

| Distribution Name | Log Likelihood | Parameter 1 | Parameter 2 |
|-------------------|----------------|-------------|-------------|
| Gamma | -5.218e+03 | 30.0053 | 1.95392 |
| Weibull | -4.985e+03 | 62.3865 | 7.9280 |
| Normal | -5.095e+03 | 58.6282 | 9.6843 |

TABLE IV- LOG LIKELIHOOD AND PARAMETERS FOR 50 °C

| Distribution Name | Log Likelihood | Parameter 1 | Parameter 2 |
|-------------------|----------------|-------------|-------------|
| Gamma | -5.292e+03 | 57.0278 | 1.4883 |
| Weibull | -5.086e+03 | 89.1486 | 10.6631 |
| Normal | -5.213e+03 | 84.877 | 10.556 |

With the environmental temperature increases, Log Likelihood and parameter values change, and lifetime can be estimated from the values. The lifetime will be changed as the parameters change. As mean and minimum junction temperatures increase, this will result in the DAF>1, leading to faster degradation.

V. EXPERIMENTAL STUDY

DC power cycling test is the most common ALT method to estimate SiC MOSFET's lifetime and degradation mechanism [19-20]. The Device Under Test (DUT) is rapidly heated by its conduction loss through high current injection, causing the junction temperature to rise to its maximum target. The DUT is then turned off and cooled to its minimum target temperature. This cycle repeats until the device degrades or fails. A forced cooling system is required to accelerate the cooling process of SiC MOSFETs.

The DC power cycling test is shown in Fig. 10. with the environment provided in Table V. FF33MR12W1M1HP_B11 SiC MOSFETs module (1200V, 25A) has been used for the degradation studies. This module is CoolSiC™ MOSFET half-bridge module 1200V. The degradation circuit is a bridge inverter consisting of a DC link capacitor, DC supply, and a half-bridge SiC MOSFET module with a resistive load. A gate driver with differential transceiver, TMS320F28335, and code composer studio software (CCS) were used to run the SiC module. The TMS320F28335 microcontroller from Texas Instruments generates all the control signals. A relay connected to Arduino has been used to automate the degradation. From the temperature sensing circuit, junction temperature are taken as feedback, and the cooling fan has been on/off based on the feedback. Three sensing circuits (Current, voltage, and temperature) extract the parameter. $R_{ds,ON}$ is measured by dividing on-state voltage and load current. $V_{ds,ON}$ is measured by the voltage sensing circuit when DUT is operating in the forward MOSFET mode.

$$R_{ds,ON} = \frac{V_{ds,ON}}{I_d} \quad (12)$$

The temperature sensing circuit is connected to the module's NTC pin, enabling precise measurement of T_j within the module. A data logger is also used to measure case temperature. At the beginning of this stage, when the junction temperature of SiC MOSFETs is the minimum temperature, the on-state resistance is measured to exclude the effect of temperature. The NI DAQ 9252 data acquisition system has been used to store $V_{ds,ON}$, T_j , and I_d . LabVIEW software is used for the NI DAQ. The data has been stored in CSV file format by LabVIEW software.

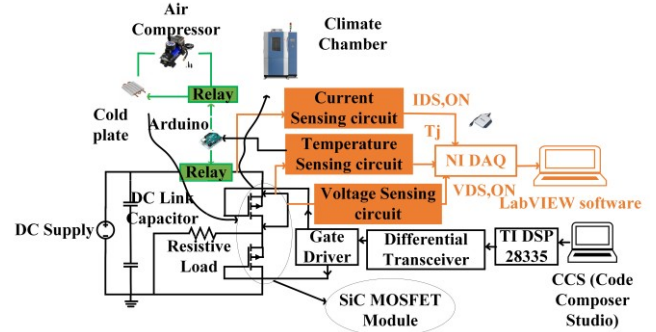


Fig. 10. Power cycling testbed with measurement circuits.

TABLE V. POWER CYCLING TESTING ENVIRONMENT

| Parameters | Symbol | Value |
|----------------------------|------------------|-----------|
| Load Current | I_{load} | 25 A |
| Load | R_{load} | 0.2 ohm |
| Gate-source Voltage | V_{GS} | -5/+20 V |
| Junction Temperature Swing | ΔT_j | 25~175 °C |
| Heating time/Cooling time | T_{on}/T_{off} | 50s/60s |

The test has been categorized into three groups. First, it is done at a controlled room ambient temperature (25°C), as shown in Fig. 11. The constant voltage mode of the DC supply is set to 8V while the constant current mode is set to 25A. The experiment utilizes a power cycling test with a temperature deviation of 25°C and 175°C, resulting in a total temperature swing (ΔT_j) of 150°C. Each cycle comprises a 50-second heating phase followed by a 60 second cooling phase.

Fig. 11. Testbed of power cycling test at the controlled environment chamber.

In the second group, the test is meticulously conducted in the climate chamber at a precisely controlled temperature of 40°C. This ensures that the minimum junction temperature is 40°C, and the maximum is 190°C, maintaining a consistent junction temperature swing (ΔT_j) of 150°C. In the last group, the test is also done in the climate chamber at a controlled temperature (50°C) with the same junction temperature swing. The minimum and maximum temperatures are 50°C and 200°C. The last two groups keep the same constant current mode of 25A and the same load conditions.

VI. RESULT AND DISCUSSION

The temperature sensing circuit is implemented through a resistor with the negative-temperature-coefficient (NTC) pin of SiC MOSFET to determine junction temperature. This NTC pin with a series resistor offer a voltage divider form, and the output voltage is linear over the junction temperature. Fig. 12 shows the temperature sensing circuit, where OPA2330AID op-amp is used for the linear output swing from 0.05V to 3.25V. Fig. 13 shows the calibration curve from the NTC pin, which indicates a high linearity between the output voltage from the NTC pin and junction temperature. The output voltage rises from 0.05V to 3.25V, and the junction temperature linearly increases from

25°C to 175°C. Fig. 14 shows the experimented output voltage data from the NTC pin and junction temperature during heat-up and cooling.

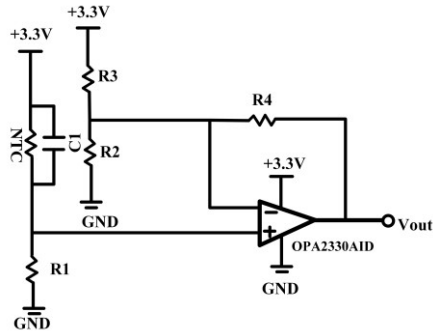


Fig. 12. Temperature sensing circuit.

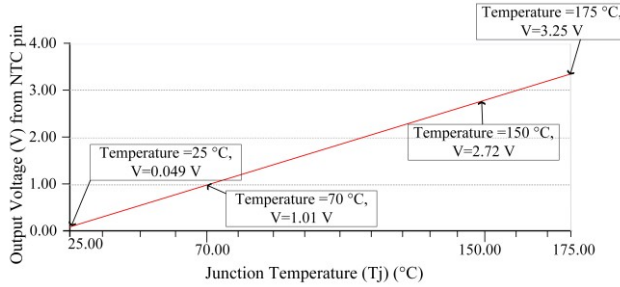


Fig. 13. Output Voltage from NTC pin vs Junction Temperature

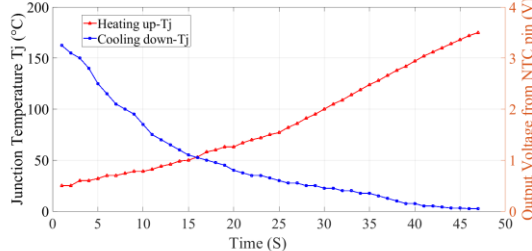


Fig. 14. Output Voltage from NTC pin and Junction temperature of SiC MOSFETs.

$V_{ds,on}$ and I_d are measured using a voltage sensing circuit and current sensing circuit and monitored by LabVIEW software throughout the testing process with a fixed load condition of 8V and its minimum junction temperature condition. The experimental data is taken from the DUT of the upper switch of the SiC Module. On-state resistance exhibits a gradual increase before device failure. Figs. 15-17 show on-state resistance for the environmental conditions of 25°C, 40°C, and 50 °C under the same load conditions. The failure threshold is assumed to be 20% of the initial resistance, showing a tight correlation between environmental temperature and the failure time.

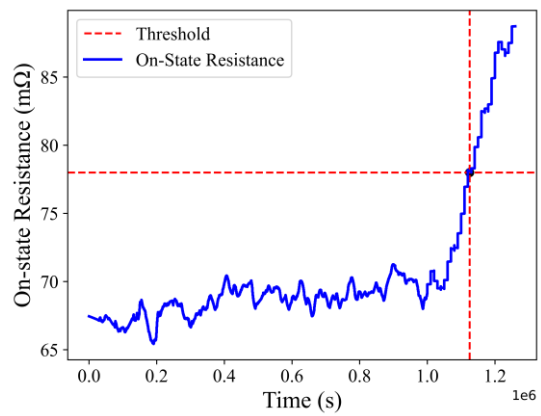


Fig. 15. $R_{ds,on}$ experimental value with power cycling test at room temperature (25°C).

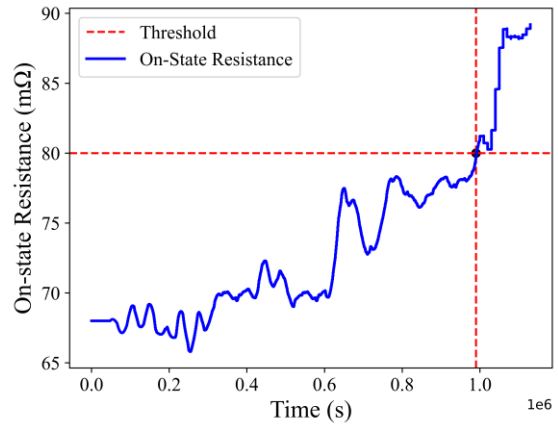


Fig. 16. $R_{ds,on}$ experimental value with power cycling test at 40°C temperature.

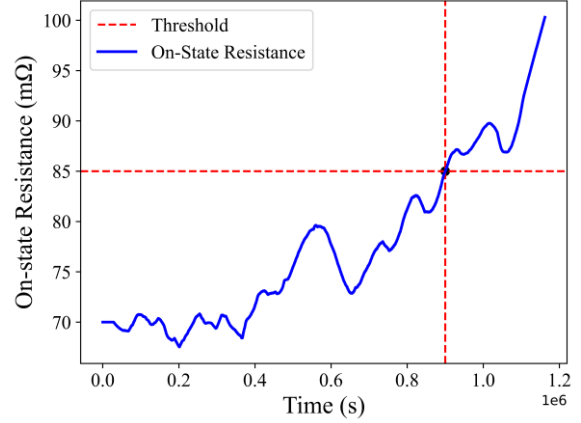


Fig. 17. $R_{ds,on}$ experimental value with power cycling test at 50°C temperature

The increase in $R_{ds,on}$ may be due to bond wire cracking and lifting off. Microscopic images are given in Fig. 18a and 18b to ensure the reason behind the degradation of SiC MOSFETs. In this case, the heel crack is the reason for the degradation of SiC MOSFETs; thus, the bond wire resistance increases, ultimately increasing the on-state resistance.

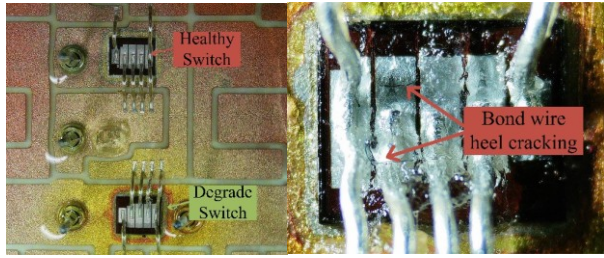


Fig. 18. (a) Healthy and Degraded switch and (b) Bond wire heel cracking.

These experimental data are used to predict through AR and ARIMA models. The testing data are taken in the high non-linearity state of $R_{ds,on}$ data. The training, testing, and prediction results for all these switches are shown in Fig. 19.

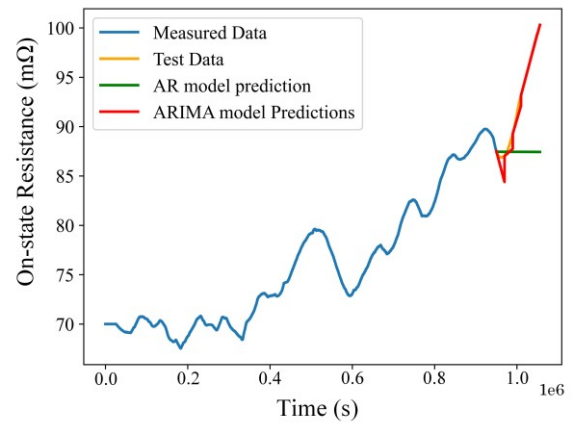
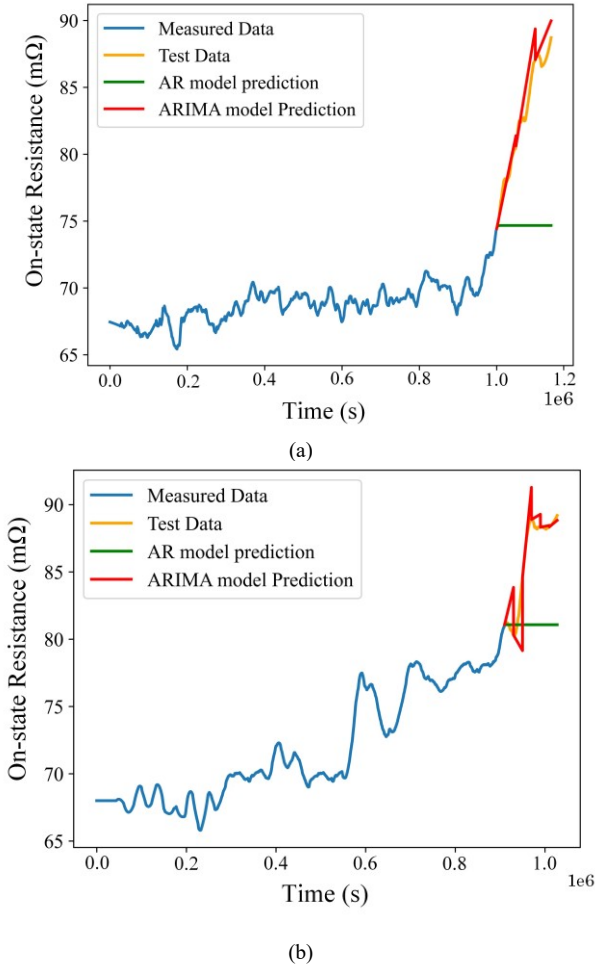


Fig. 19. AR and ARIMA model prediction of $R_{ds,on}$ experimental value at (a) 25°C, (b) 40°C, and (c) 50°C temperature.

The predictions in the ARIMA model are very close to the measured values. The ARIMA model gives better predictions than the AR model in the high non-linearity state. Table VI represents the RMSE value for these two models for the three experimental values of $R_{ds,on}$.

| TABLE VI- RMSE VALUES OF AR AND ARIMA MODELS | | | |
|--|-----------------------|------|--------------|
| Conditions | Performance indicator | AR | ARIMA |
| 25°C | RMSE of Predictions | 9.02 | 1.25 |
| | | 5.85 | 1.44 |
| | | 6.55 | 0.747 |

The ARIMA-based prediction method proposed better accuracy than the AR model for predicting the changes of the precursor of SiC MOSFET with the device aging through the measured data.

VII. CONCLUSION

In this paper, the impact of real-world environmental thermal conditions on T_j has been integrated into precise RUL prediction based on the $R_{ds,on}$ of SiC MOSFETs. Initial simulation shows that environmental factors, particularly temperature, could significantly influence the operating T_j , resulting in large RUL errors. This critical correlation has been thoroughly explored under various temperature conditions within a climate chamber, and a detailed mathematical model has been derived. The new findings have been integrated. This comprehensive research and the resulting RUL estimation method, incorporating real-world environmental conditions, could be a reliable and practical tool in many energy system applications.

ACKNOWLEDGMENT

This work was supported in part by the NSF Electrical, Communications and Cyber Systems (ECCS) Program under Award 2210106.

REFERENCES

[1] Stella, F., Pellegrino, G., Armando, E., & Daprà, D., "Online junction temperature estimation of SiC power MOSFETs through on-state voltage mapping," IEEE Transactions on Industry Applications, 2018, 54(4), 3453-3462.

[2] Qin, MIL-HDBK-217F-N2, "Reliability Prediction of Electronic Equipment", Washington: US Department of Defense, 1995, 80 p.

[3] Li, H., Wang, Y., Zhao, X., Sun, K., Zhou, Z., & Xu, Y., "A junction temperature-based PSpice short-circuit model of SiC MOSFET considering leakage current," IECON 45th Annual Conference of the IEEE Industrial Electronics Society, Vol. 1, pp. 5095-5100, 2019.

[4] Y. Wang, E. Deng, L. Wu, Y. Yan, Y. Zhao, and Y. Huang, "Influence of Humidity on the Power Cycling Lifetime of SiC MOSFETs," in IEEE Transactions on Components, Packaging and Manufacturing Technology, vol. 12, no. 11, pp. 1781-1790, Nov. 2022, doi: 10.1109/TCMPT.2022.3223957.

[5] Baker, N., Liserre, M., Dupont, L., & Avenas, Y., "Improved reliability of power modules: A review of online junction temperature measurement methods," IEEE Industrial Electronics Magazine, 2014, 8(3), 17-27.

[6] X. Ding, B. Wang and Y. Yang, "DC Power Cycling Test and Lifetime Prediction for SiC MOSFETs," 2023 26th International Conference on Electrical Machines and Systems (ICEMS), Zhuhai, China, 2023, pp. 4638-4643, doi: 10.1109/ICEMS59686.2023.10344327

[7] M. S. Haque and S. Choi, "Prognosis of enhance mode gallium nitride high electron mobility transistors using on-state resistance as fault precursor," 2017 IEEE Energy Conversion Congress and Exposition (ECCE), Cincinnati, OH, USA, 2017, pp. 1988-1994, doi: 10.1109/ECCE.2017.8096400.

[8] M. S. Haque, J. Baek, J. Herbert and S. Choi, "Prognosis of wire bond lift-off fault of an IGBT based on multisensory approach," 2016 IEEE Applied Power Electronics Conference and Exposition (APEC), Long Beach, CA, USA, 2016, pp. 3004-3011, doi: 10.1109/APEC.2016.7468291.

[9] A. Rahnama Sadat and H. Sarma Krishnamoorthy, "Measure Theory-based Approach for Remaining Useful Lifetime Prediction in Power Converters," 2020 IEEE Energy Conversion Congress and Exposition (ECCE), Detroit, MI, USA, 2020, pp. 2541-2547, doi: 10.1109/ECCE44975.2020.9235635.

[10] X. Han and M. Saeedifard, "Junction temperature estimation of SiC MOSFETs based on Extended Kalman Filtering," 2018 IEEE Applied Power Electronics Conference and Exposition (APEC), San Antonio, TX, USA, 2018, pp. 1687-1694, doi: 10.1109/APEC.2018.8341244.

[11] F. Stella, G. Pellegrino, E. Armando and D. Daprà, "Online Junction Temperature Estimation of SiC Power MOSFETs Through On-State Voltage Mapping," in IEEE Transactions on Industry Applications, vol. 54, no. 4, pp. 3453-3462, July-Aug. 2018, doi: 10.1109/TIA.2018.2812710.

[12] M. S. Haque, S. Choi and J. Baek, "Auxiliary Particle Filtering-Based Estimation of Remaining Useful Life of IGBT," in IEEE Transactions on Industrial Electronics, vol. 65, no. 3, pp. 2693-2703, March 2018, doi: 10.1109/TIE.2017.2740856.

[13] D. Qin, G. Ozkan, C. Edrington and Z. Zhang, "Electrothermal Management Using In-situ Junction Temperature Monitoring for Enhanced Reliability of SiC-Based Power Electronics," 2021 IEEE Electric Ship Technologies Symposium (ESTS), Arlington, VA, USA, 2021, pp. 1-7, doi: 10.1109/ESTS49166.2021.9512370.

[14] M. Moniruzzaman, A. H. Okilly, S. Choi, J. Baek, T. I. Mannan and Z. Islam, "A Comprehensive Study of Machine Learning Algorithms for GPU based Real-time Monitoring and Lifetime Prediction of IGBTs," 2024 IEEE Applied Power Electronics Conference and Exposition (APEC), Long Beach, CA, USA, 2024, pp. 2678-2684, doi: 10.1109/APEC48139.2024.10509167.

[15] W. Zhou, X. Zhong and K. Sheng, "High Temperature Stability and the Performance Degradation of SiC MOSFETs," in IEEE Transactions on Power Electronics, vol. 29, no. 5, pp. 2329-2337, May 2014, doi: 10.1109/TPEL.2013.2283509.

[16] Wu W, Gu Y, Yu M, Gao C, Chen Y. Remaining Useful Lifetime Prediction Based on Extended Kalman Particle Filter for Power SiC MOSFETs. *Micromachines* (Basel). 2023 Apr 12;14(4):836. doi: 10.3390/mi14040836.

[17] Z. Ni, X. Lyu, O. P. Yadav, B. N. Singh, S. Zheng and D. Cao, "Overview of Real-Time Lifetime Prediction and Extension for SiC Power Converters," in IEEE Transactions on Power Electronics, vol. 35, no. 8, pp. 7765-7794, Aug. 2020, doi: 10.1109/TPEL.2019.2962503.

[18] Z. Ni, X. Lyu, O. P. Yadav and D. Cao, "Review of SiC MOSFET based three-phase inverter lifetime prediction," 2017 IEEE Applied Power Electronics Conference and Exposition (APEC), Tampa, FL, USA, 2017, pp. 1007-1014, doi: 10.1109/APEC.2017.7930819.

[19] F. Yang, E. Ugur and B. Akin, "Design Methodology of DC Power Cycling Test Setup for SiC MOSFETs," in IEEE Journal of Emerging and Selected Topics in Power Electronics, vol. 8, no. 4, pp. 4144-4159, Dec. 2020, doi: 10.1109/JESTPE.2019.2914419.

[20] L. R. GopiReddy, L. M. Tolbert and B. Ozpineci, "Power Cycle Testing of Power Switches: A Literature Survey," in IEEE Transactions on Power Electronics, vol. 30, no. 5, pp. 2465-2473, May 2015, doi: 10.1109/TPEL.2014.2359015.